Nonlinear Dynamic Analysis of RC Frame under Earthquake Loading

H. G. Kwak
E. Oñate
S.P. Kim

Publication CIMNE Nº-229, July 2003

Nonlinear Dynamic Analysis of RC Frame under Earthquake Loading

H.G. Kwak
E. Oñate
S.P. Kim

Publication CIMNE Nº-229, July 2003

International Center for Numerical Methods in Engineering
Gran Capitán s/n, 08034 Barcelona, Spain

Nonlinear Dynamic Analysis of RC Frame under Earthquake Loading

H.G. Kwak [a], Eugenio Oñate [b] and S.P. Kim [c]

[a] Associate Professor, Dept. of Civil and Environmental Engineering, Korea Advanced Institute of Science and Technology, 373-1 Guseong-dong, Yuseong-gu, Daejeon 305-701, KOREA

[b] Professor, International Centre for Numerical Methods in Engineering, Unversidad Politecnica de Cataluna, Gran Capitan sln, 08034 Barcelona, Spain

[c] PhD. Student, Dept. of Civil and Environmental Engineering, Korea Advanced Institute of Science and Technology, 373-1 Guseong-dong, Yuseong-gu, Daejeon 305-701, KOREA

Abstract

Nonlinear dynamic analysis of a reinforced concrete (RC) frame under earthquake loading is performed in this paper on the basis of a hysteretic moment-curvature relation. Unlike previous analytical moment-curvature relations which take into account the flexural deformation only with the perfect-bond assumption, the proposed relation considers the rigid-body-motion due to anchorage slip at the fixed end, which accounts for more than 50% of the total deformation, using an equivalent flexural stiffness. The advantage of the proposed relation, compared with the layered section approach and multi-component model, may be on the easiness in application to a complex structure composed of many elements and on the reduction in calculation time and memory space. The use of curved unloading and reloading branches inferred from the stress-strain relation of steel and consideration of the pinching effect caused by axial force make it possible to describe the structural response more exactly. Finally, correlation studies between analytical and experimental results are conducted to establish the applicability of the proposed model to the nonlinear dynamic analysis of RC structures.

Keywords: RC Frame, Earthquake Loading, Anchorage Slip, Pinching Effect, Bauschinger Effect, Moment-Curvature Relationship

1 Introduction

Since the first introduction of a bilinear moment-curvature relation by Clough and Johnson [2] the various mechanical models for the hysteretic moment-curvature relation have been introduced to analyze the behavior of RC beams subject to cyclic loadings. Such models include cyclic stiffness degradation and further modifications to take into consideration the pinching effect due to the shear force and the strength degradation after yielding of steel. In addition, by using the bilinear hysteretic curve instead of trilinear, a more simplified model has been proposed. Nevertheless, these models still have limitations in simulating exact structural behavior of RC columns because of the exclusion of the bond-slip, fixed-end rotation effect, axial force and Bauschinger effect. On these backgrounds, a curved hysteretic moment-curvature relation is introduced. Unlike the previously proposed models, the bond-slip and fixed-end rotation effect are taken into account by defining the initial loading branch on the basis of the monotonic moment-curvature relation considering these effects. The following curved hysteretic unloading and reloading branches are defined, and the pinching effect caused by the axial force is also taken into consideration. The validity of the proposed model is established by comparing the analytical predictions with results from experimental and previous analytical studies.

2 Proposed Moment-Curvature Relation

The proposed model can basically be divided into four different regions.

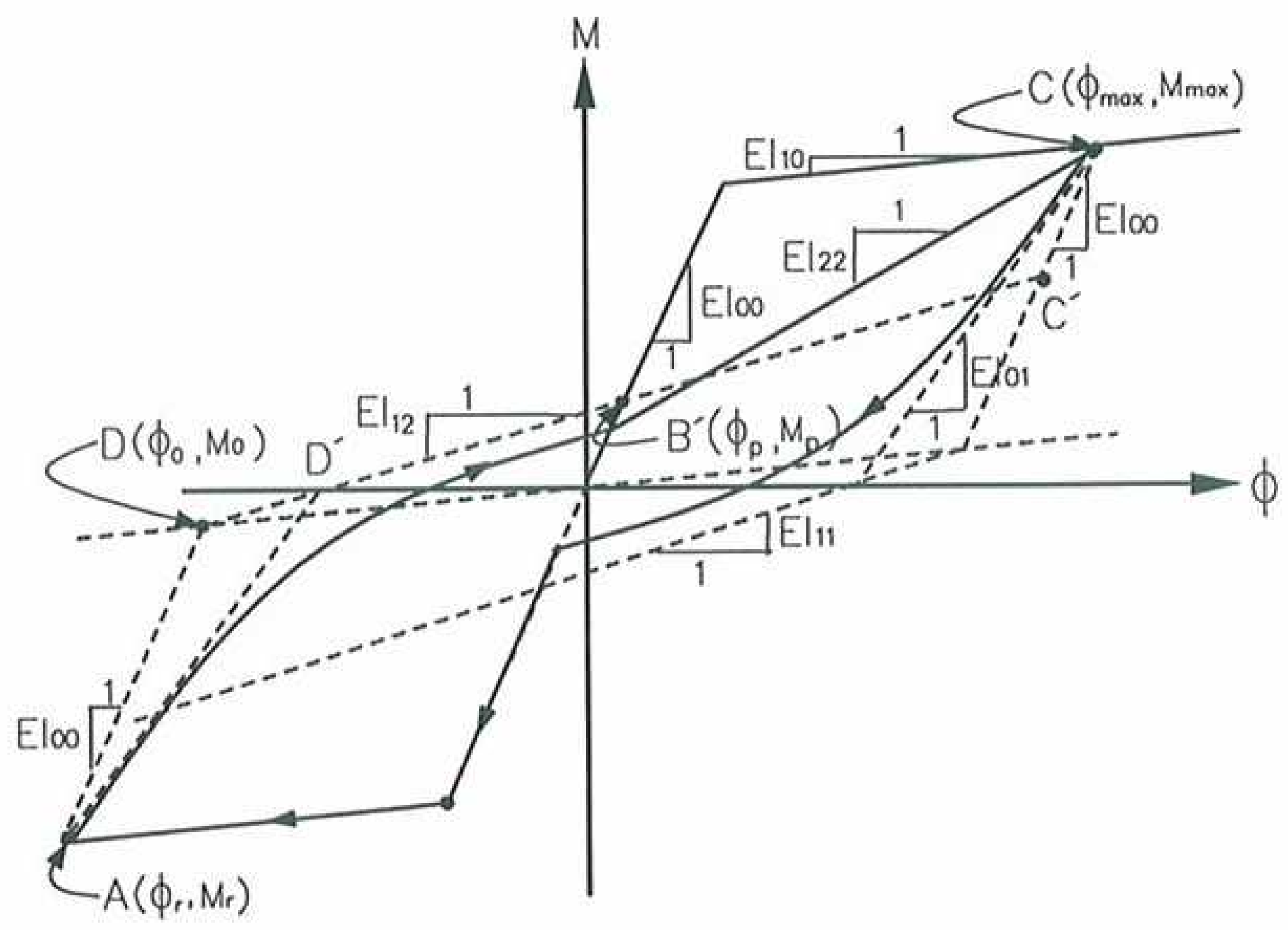

Figure 1 : Proposed Moment-Curvature Relationship

Region 1 (an initial elastic branch with stiffness EI_{00} in Figure 1) : Unlike the previously introduced hysteretic models, the bond-slip effect and fixed-end rotation effect are already taken into consideration while defining the initial stiffness EI_{00} in Figure 1.

Region 2 (curved region of point A to point B in Figure 1) : In this region, moment-curvature curve is assumed with following relation:

$$M^* = p \cdot \phi^* + \frac{(1-p)\cdot \phi^*}{\left(1+\phi^{*G}\right)^{\frac{1}{G}}} \qquad \phi^* = \frac{\phi - \phi_r}{\phi_0 - \phi_r}, \; M^* = \frac{M - M_r}{M_0 - M_r} \tag{1}$$

where the hardening parameter p is changed according to the loading history and assumed to have the ratio between a slope EI_{0i} which represents a modified flexural stiffness of the initial elastic stiffness EI_{00} and EI_{1i} which means the slope of a straight line connecting the point D(ϕ_0, M_0) and the point C($\phi_{\max}$, $M_{\max}$) at the *i-th* load reversal. The points D(ϕ_0, M_0) and A(ϕ_r, M_r) will be updated after each curvature reversal.

Region 3 (linear region from point B to point C in Figure 1) : Since the structural behavior in this region represents the proportional increment of the load carrying capacity, the moment-curvature curve is assumed with the following linear relation

$$M = EI_{2i} \cdot \phi + (M_{\max} - EI_{2i} \cdot \phi_{\max}) \tag{2}$$

where EI_{2i} is the slope of straight-line connecting the points B(ϕ_n', M_n') and C($\phi_{\max}$, $M_{\max}$) at the *i-th* load reversal.

Region 4 (yielding region after the point C in Figure 1) : The second branch of the primary moment-curvature curve can be expressed as

$$M = EI_{10} \cdot \phi + (M_{\max} - EI_{10} \cdot \phi_{\max}) \tag{3}$$

where EI_{10} is flexural stiffness of monotonic envelope after yielding.

3 Modification of Moment-Curvature Relation

3.1 Axial Force Effect on Moment-Curvature Relation

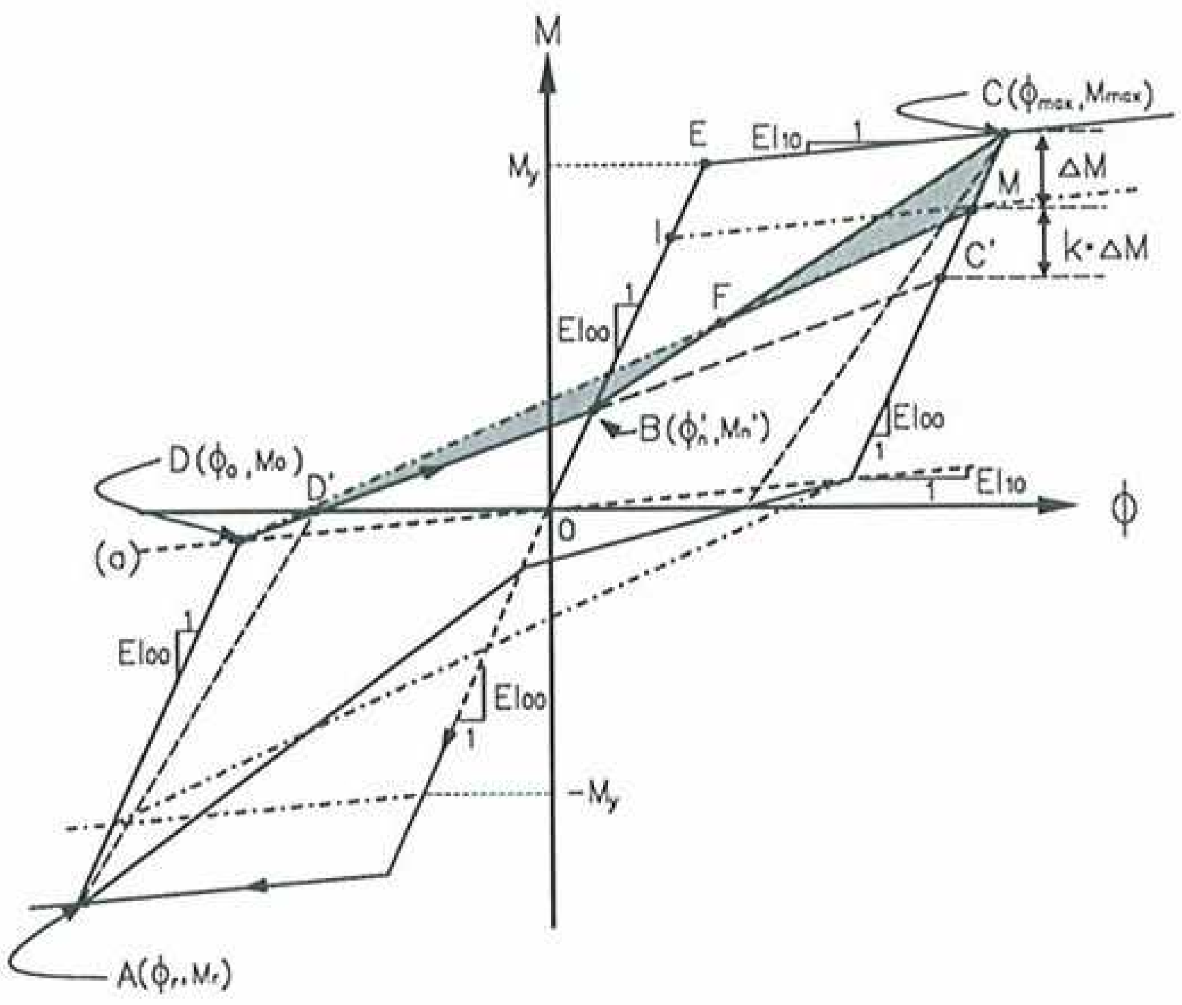

Figure 2 : Considering the axial force effect

When a RC column is subject to an axial load P, the ultimate resisting moment M increases almost proportionally to the axial load P until the RC section reaches the balanced failure point in the $P-M$ intersection diagram. In advance, as well known through the experimental studies [5,8,12], the hysteretic moment-curvature relation of a RC section subject to an axial load represents a marked pinching of loops because the axial force acts to close open cracks and causes a sudden increase in stiffness after crack closing. To reflect the axial force effect into a hysteretic moment-curvature relation, modifications of the monotonic skeleton curve and of the unloading and reloading branches are required. Firstly, the monotonic skeleton moment-curvature curve for a RC beam ($\overline{OEC}$ in Figure 2) proposed by Kwak and Kim [4] in which bond-slip effect and fixed-end rotation effect are taken into consideration needs to be modified to include an axial force effect. If it is assumed that the line $\overline{OIM}$ in Figure 2 corresponds to the monotonic skeleton curve and the line $\overline{DFM}$ in Figure 2 to the straight line asymptote for the beam without an axial force, respectively, then the modified asymptote $\overline{DBC}$ in Figure 2 can be constructed on the basis of the energy equilibrium condition. Since the external work by an axial force lower than the balanced load P_b can be ignored due to the negligibly small axial deformation, the internal energy represented by the area within the hysteretic loop must maintain a constant value regardless of the applied force. This implies that the area of the triangle ΔDBF will be the same as that of the triangle ΔFMC in Figure 2. Point B in Figure 2 which defines the modified crack closing point, is finally determined through the calculation of the constant k in Figure 2. When the constant k is represented by $k = (M_m - M_{c'})\ /(M_{\max} - M_m)$, it can be simplified as the following equation from the area equality of two triangles ($\Delta DBF = \Delta FMC$):

$$k = \frac{M_y - M_{\max}}{M_0} \tag{4}$$

3.2 Consideration of Fixed-End Rotation

The behavior of the critical region at the beam-column joint of relatively short-span beams may be greatly affected both by the shear and also by the details of anchoring the beam reinforcements. In particular, slippage of the main bars from the anchorage zone accompanies the rotation of the beam fixed-end, θ_{fe}, which cannot be simulated with any mechanical model, and this rigid body deformation may be increased as the deformation increases. To account for the fixed-end rotation in the numerical analyses, it is common to reduce the stiffness, EI, in the moment-curvature relation for the elements located at the ends of beam with the range of the plastic hinge length(see Figure 3 (b) and Figure 4). If a beam with the rotational stiffness k_θ at both ends is subjected to a horizontal force P, as shown in Figure 3 (a), the corresponding horizontal drift Δ_1 can be obtained.

$$\Delta_1 = \frac{PL^3}{12EI} + \frac{PL^2}{2k_\theta} \tag{5}$$

Where the first term means the contribution by the bending deformation of the beam and the second term by the end rotational stiffness k_θ.

When the same force acts on a beam with the reduced stiffness EI_{eq} at the both ends, as shown in Figure 3 (b), the horizontal deflection Δ_2 also can be calculated by the moment area method. From the equality condition of $\Delta_1 \equiv \Delta_2$, the equivalent stiffness EI_{eq} can be determined by

$$\frac{1}{EI_{eq}} = \frac{1}{\beta \cdot k_\theta \cdot L} + \frac{1}{EI} \tag{6}$$

Where $\beta = \alpha\left(1 - 2\alpha + 4/3\alpha^2\right)$, $\alpha = l_p / L$

The same derivation procedure for the cantilevered beam is applied the equivalent stiffness EI_{eq} obtained in this case ahs the same form with Eq. (6) except the parameter β has the form of $\beta = \alpha\left(1 - \alpha + 1/3\alpha^2\right)$

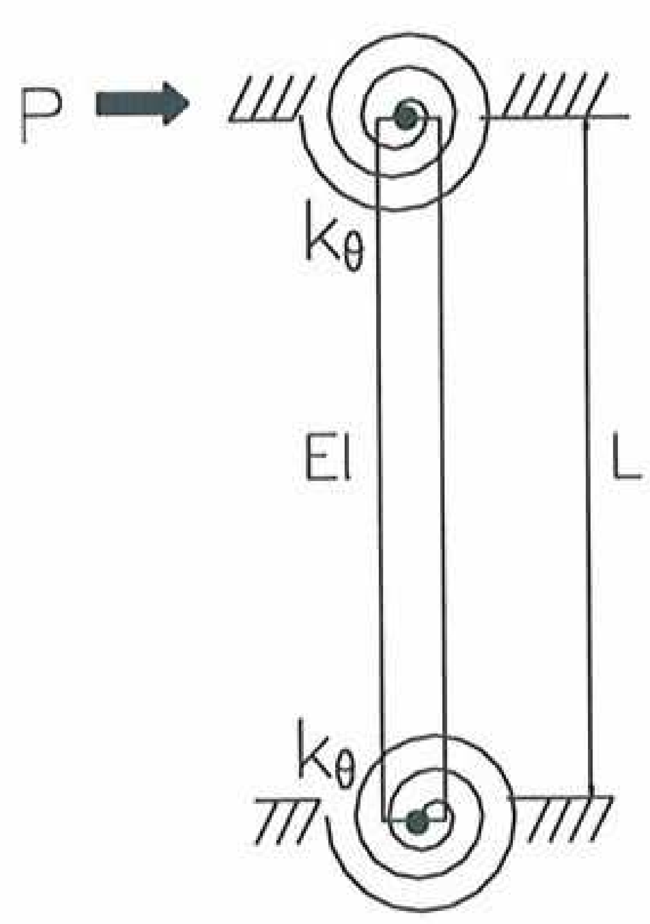

(a) Simplified Model with k_θ

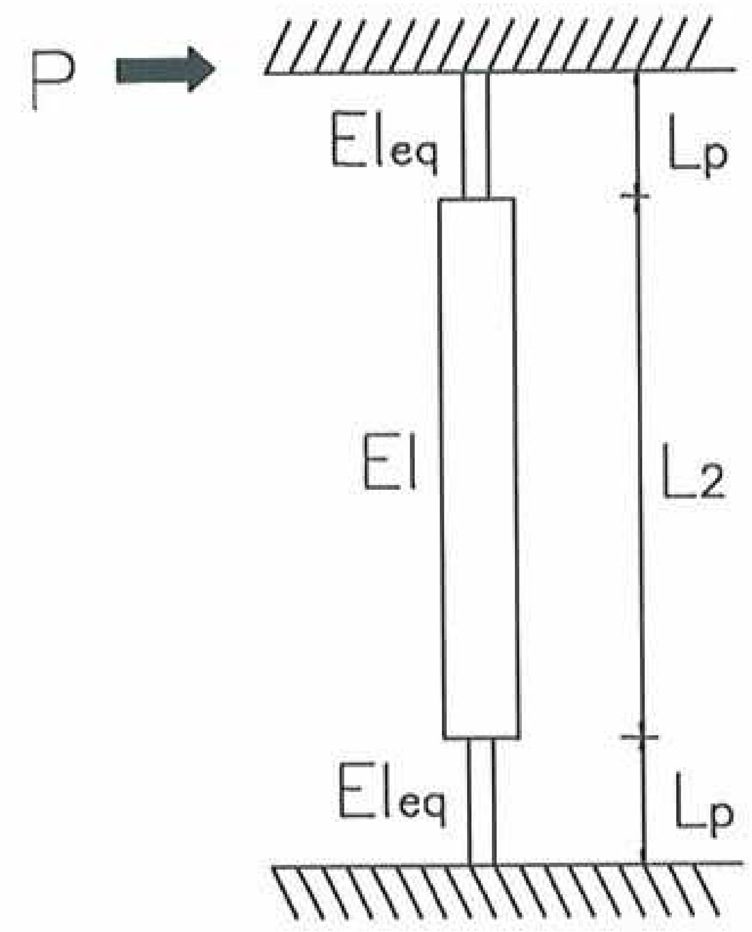

(b) A Simplified Model with EI_{eq}

Figure 3 : Consideration of the Equivalent Stiffness

From the above equation, if the stiffness ratio α_{fe} is defined by $\alpha_{fe} = EI / EI_{eq}$ the modified curvature can be expressed as $\phi' = \alpha_{fe}\phi_{flex}$ where ϕ_{flex} represent the curvature at the fixed-end of the beam due to the flexural behavior. In advance, the modified stiffness of the initial elastic branch, EI'_{00}, and that of the following inelastic branch, EI'_{10}, can be defined by $EI'_{10} = EI_{10} / \alpha_{fe}$ from the relations of $M_y = EI_{00}\phi_y = EI_{eq}\phi'_y = EI_{eq}\alpha_{fe}\phi_y$ and $M - M_y = EI_{10}\left(\phi - \phi_y\right) = EI'_{10}\left(\phi' - \phi'_y\right)$ where ϕ_y and M_y are the curvature and moment at the yielding of a section, respectively (see Figure 4).

However it is almost impossible to conduct experiments on all the beam elements used in a structure to obtain the rigid body rotation or deflection of each member. In this case, the relation between the steel stress and crack width, introduced on the basis of analytical or experimental studies, can be utilized [3,6,7,9] By assuming that a half of the crack width, when the steel yields at the laterally loaded RC beams, corresponds to the anchorage slip of the reinforcing bar, Δ_{fe}, the rotational stiffness k_θ can be defined by

$$\theta_{fe} = \frac{\Delta_{fe}}{d-c}, \quad k_\theta = \frac{M_y}{\theta_{fe}} \tag{7}$$

where c is the distance from the extreme compression fiber to the neutral axis. The neutral axis depth c maintains an almost constant value of $c = \alpha \cdot d$ from the initial cracking up to the yielding of the reinforcing steel.

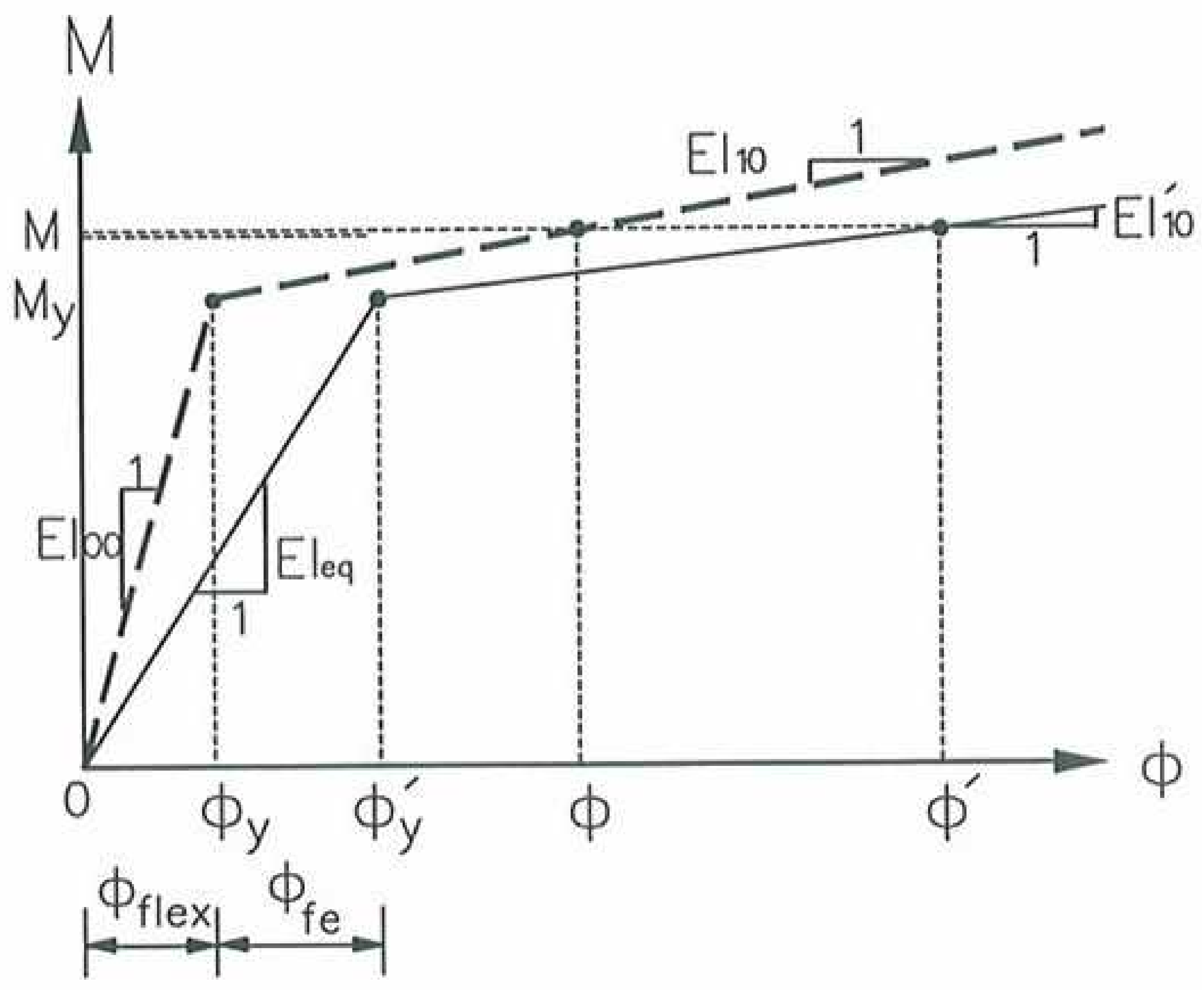

Figure 4 : Modification of Monotonic Envelope Curve

After calculation of the stiffness reduction ratio α_{fe}, the modified stiffness of the initial elastic branch and that of the inelastic branch can be calculated.. In addition, the modified stiffness EI_{eq} and EI'_{10} instead of the initial stiffness EI_{00} and EI_{10}, are used as the asymptotes in defining the subsequent unloading and reloading curves. Figure 4 shows the modified monotonic moment-curvature envelope curve.

4 Numerical Application

In order to establish the applicability of the proposed hysteretic moment-curvature relation, a RC column subject to a cyclic loading and a RC frame subject to a dynamic loading are investigated and discussed. The specimens are COLUMN2 experimented by Low and Moehle [5] and a frame (RCF2) experimented by Clough and Gidwani [1].

4.1 COLUMN2

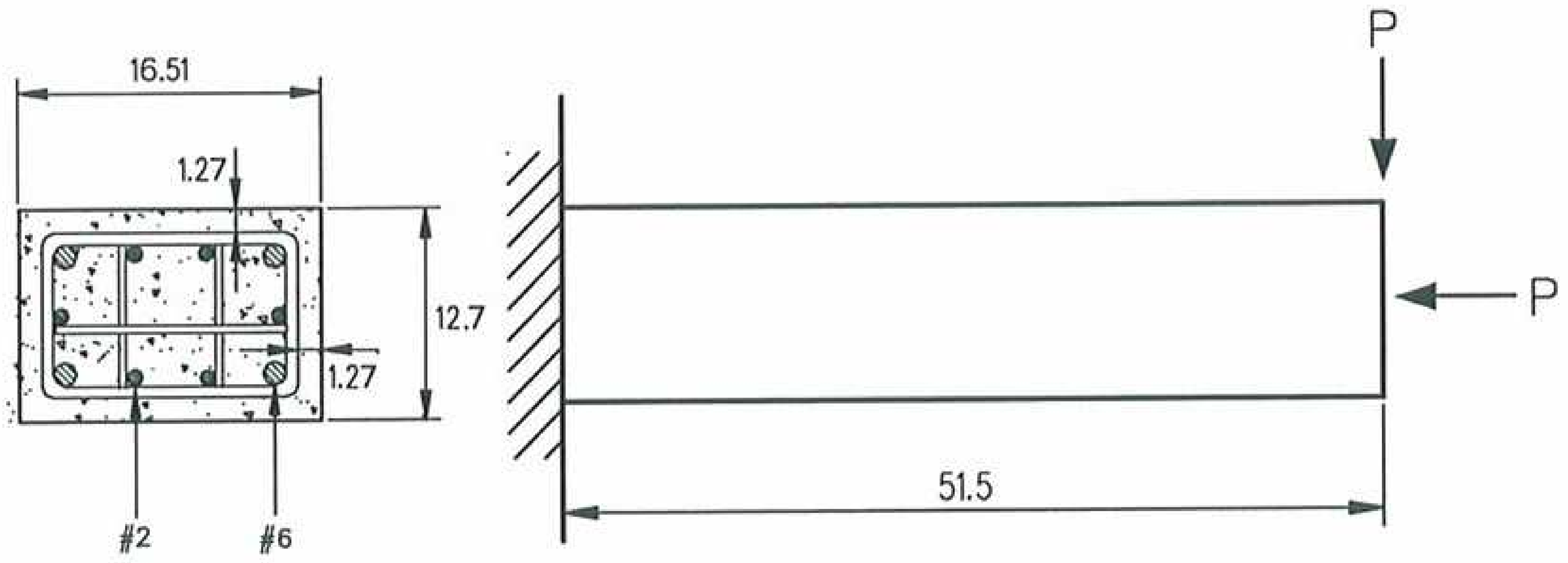

Figure 5 : Details of COLUMN2 (unit: cm)

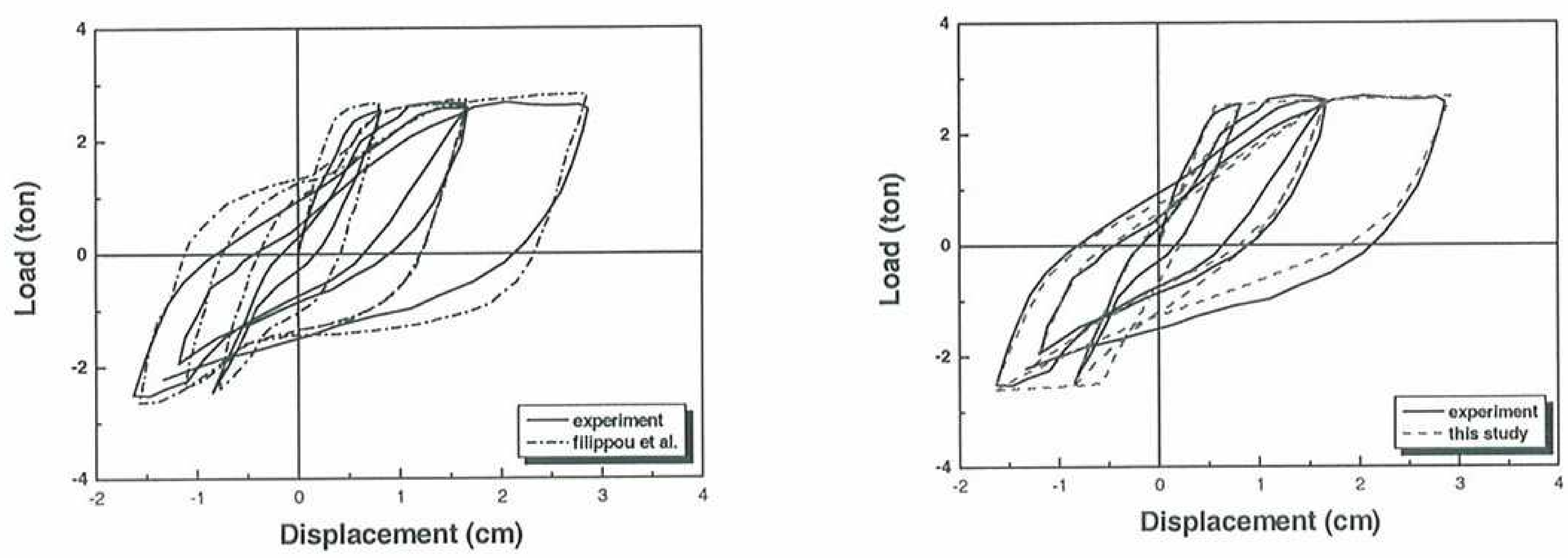

(a) Filippou et al.

(b) This study

Figure 6 : Load-Deflection Relation of COLUMN2

COLUMN2 was analyzed by Filippou et al. [11] on the basis of the layered section approach and Figure 6 shows the obtained load-deflection relation. The numerical results by Filippou et al. also simulate the ultimate resisting capacity effectively because the axial force effect is included in their formulation by considering the axial force equilibrium condition on a section. However, the layered section approach represents slightly stiffer structural behavior than the experimental data. This difference seems to be caused by ignoring the bond-slip effect and fixed-end rotation. Since the layered section approach is based on equilibrium and compatibility conditions between each imaginary layer, the bond-slip effect cannot be taken into account, and unrealistic stiffer structural behavior deepens as the deformation increases, following overestimation of the energy absorbing capacity of a structure. Especially, the stiffness degradation is generally accompanied by a decrease of shear stiffness as the deformations increase. However, the layered section approach has a limitation in simulating this phenomenon because it is basically based on the bending behavior. On the other hand, the proposed model effectively simulates the stiffness degradation and pinching phenomenon caused by the application of axial load. This result seems to be arisen from the fact that the bond-slip effect and fixed-end rotation have already been included during construction of the monotonic skeleton curve of the moment-curvature relation.

4.2 RCF2

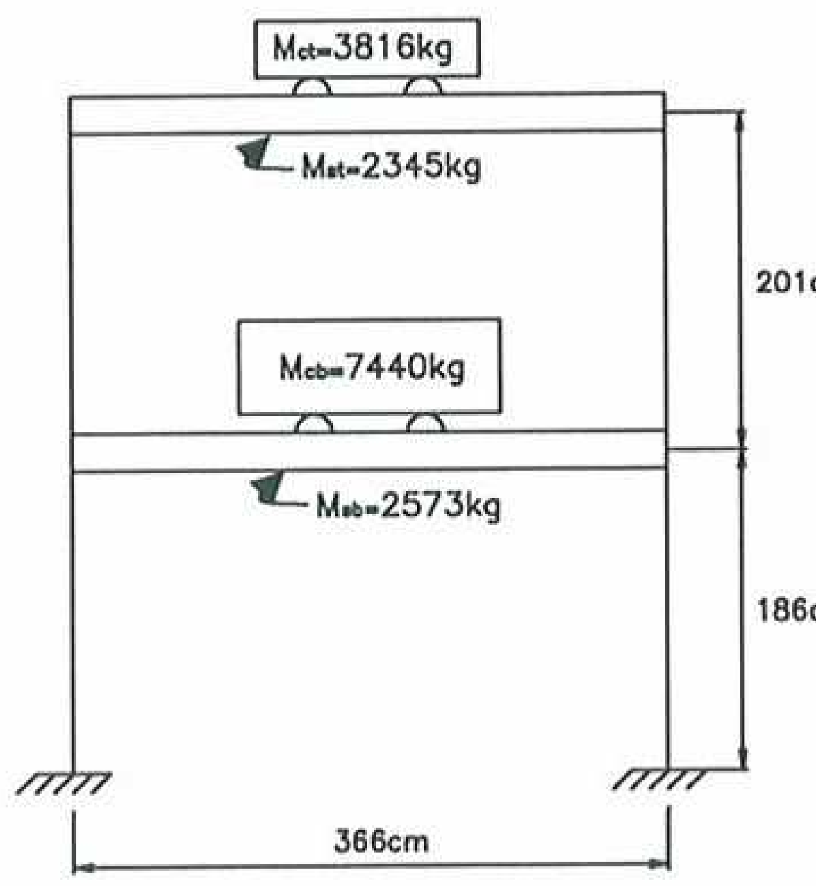

Figure 7 : Ideal Model of RCF2

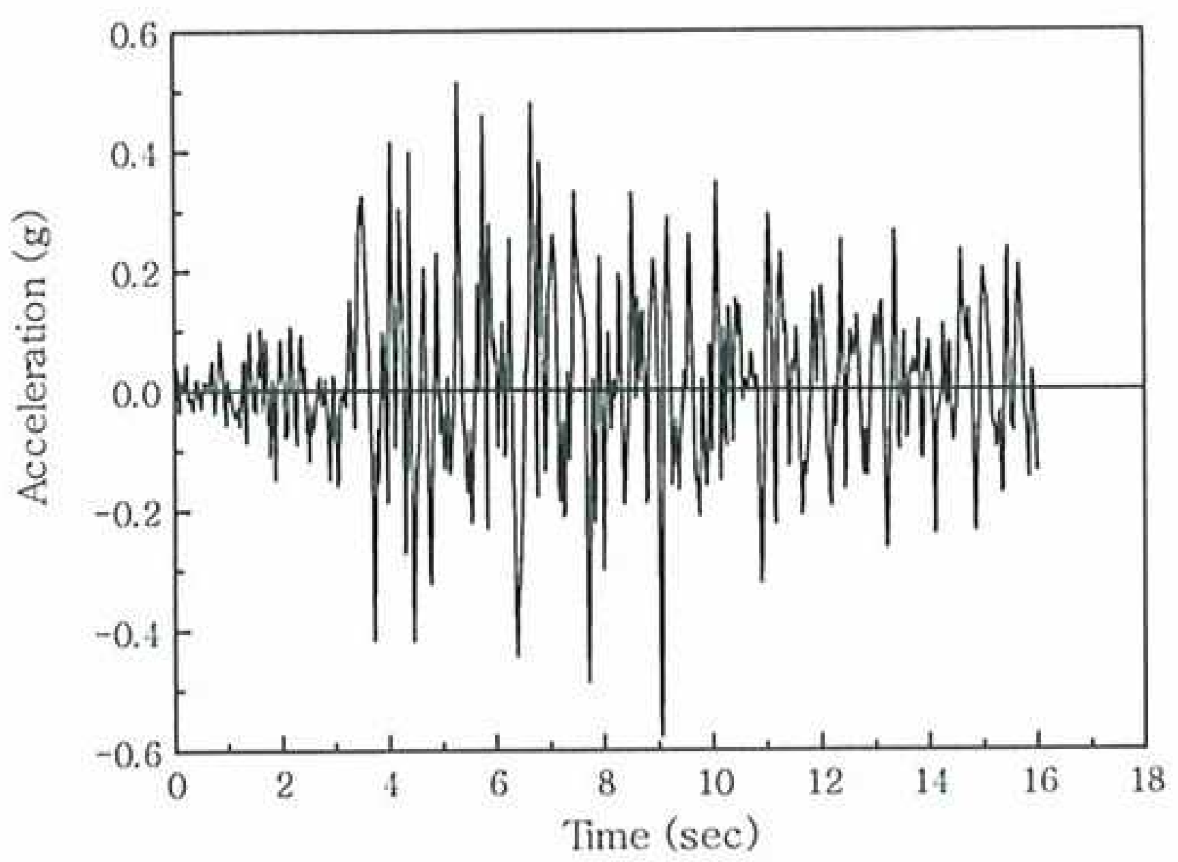

Figure 8 : Input Accelerogram Record

Figure 9 and Figure 10 show the final numerical result of RCF2 at the bottom story. As shown in Figure 9 and Figure 10, a direct application of the Takeda model [10], which was designed for a beam element without an axial load, leads to an incorrect structural response. The difference between the Takeda model and the experimental data seems to be caused by the linearized approximation of unloading and reloading curves and by not considering the bond slip effect and fixed-end rotation. In addition, the classical hysteretic moment-curvature relations for the beam element do not take into account the increase of the ultimate resisting moment and the pinching phenomenon due to the axial load. On the other hand, the proposed model effectively estimates the ultimate resisting capacity and simulates the pinching phenomenon even at the large deformation stage. Accordingly, a more exact prediction of structural responses for RC columns and/or prestressed concrete beams subject to an axial force explains the importance of the axial force effect indirectly.

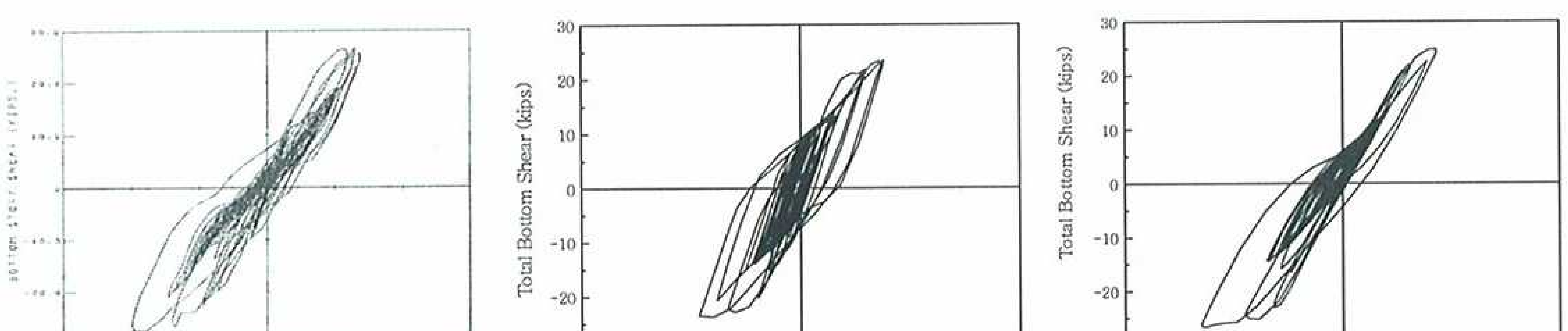

(a) Experiment (b) Takeda model (c) This study

Figure 9 : Load-Deflection Relation of RCF2 at the Bottom Story

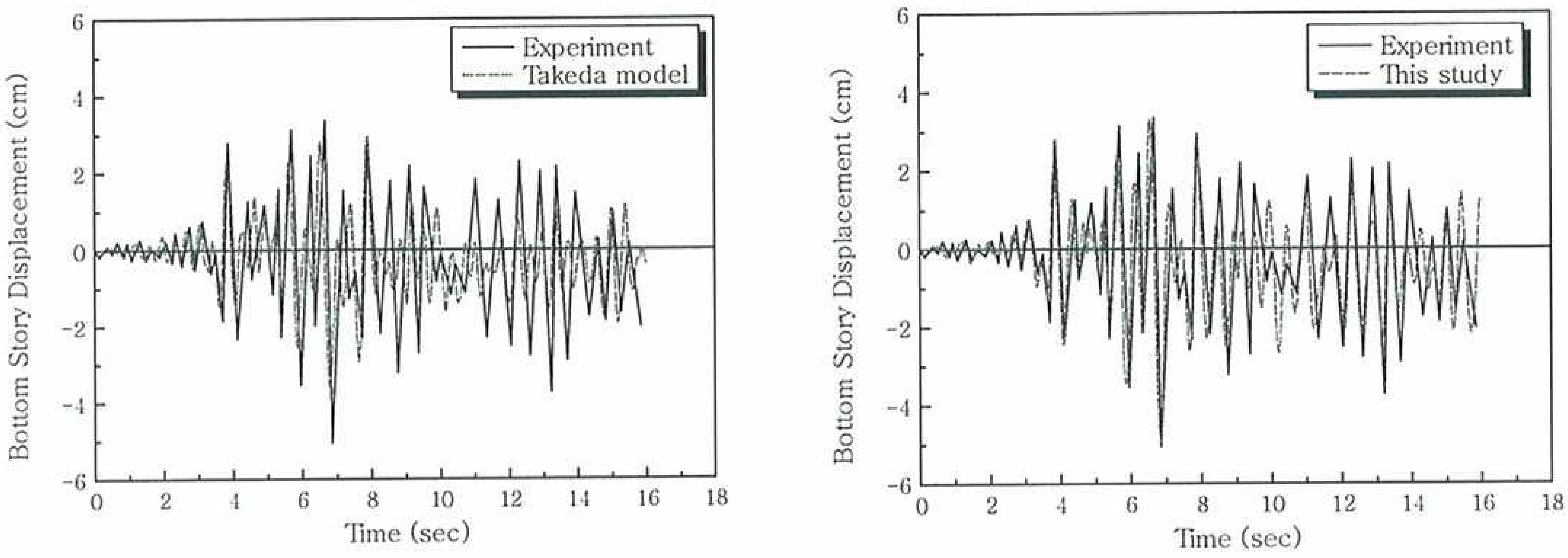

(a) Takeda model (b) This study

Figure 10 : Time-Displacement Relation of RCF2 at the Bottom Story

5 Conclusion

The present study concentrates on the introduction of a moment-curvature relation of a RC section that can simulate the cyclic behavior of RC columns and RC frame. Unlike most mathematical or mechanical models found in the literature, the proposed model has taken into account the bond-slip effect, Bauschinger effect of the steel, axial force effect and fixed-end rotation effect. In advance, a modification of the hysteretic moment curvature relation to consider an increase of the ultimate resisting capacity and the pinching phenomenon in the axially loaded RC columns is also introduced on the basis of the energy conservation. However, differently from many numerical and mechanical models considering the strength degradation, this effect is still not included in the proposed model. An additional concern for the strength degradation under cyclic loading beyond the yield strength may be required to estimate the exact damage level undergone by a section after a certain number of cycles. Through correlation studies between analytical results and experimental values from typical RC column tests, the following conclusions are obtained: (1) The inclusion of pinching effect is important in structures dominantly affected by an axial force; (2) to accurately predict the structural behavior of the beam to column subassemblage where the nonlinear response is concentrated, a modification of the moment-curvature relation to consider the fixed end rotation is strongly required; (3) to effectively simulate axially loaded RC columns, the axial load effect must be considered; and finally (4) the proposed model can be effectively used to predict the structural response of RC columns under cyclic loadings, and its application can be extended to the dynamic analysis of a frame structure.

References

[1] Clough, R. W. and Gidwani, J. (1976) Reinforced Concrete Frame 2 : Seismic Testing and Analytical Correlation, Earthquake Engrg. Research Center Report No. EERC 76-15, Univ. of California, Berkeley, Calif

[2] Clough, W. and Johnson, S. B. (1966) "Effect of stiffness degradation on earthquake ductility requirements", *Proceedings of Japan Earthquake Engineering Symposium*, October.

[3] HARAJLI M. H. and MUKADDAM M. A. Slip of steel bars in concrete joints under cyclic loading, Journal of Structural Engineering, ASCE, 1988, 114(9), 2017-2039.

[4] Kwak, H. G., and Kim, S. P. (2001) Nonlinear Analysis of RC Beam Subjeded to Cyclic Loading, *Journal of Structural Engineering, ASCE*, 127(12), pp. 1436-1444.

[5] Low, S. S. and Moehle, J. P. (1987) "Experimental study of reinforced concrete columns subjected to multi-axial cyclic loading", *Earthquake Engrg. Research Center Report No. EERC 87-14*, Univ. of California, Berkeley, Calif.

[6] MONTI G., FILIPPOU F. C. and SPACONE E. Analysis of hysteretic behavior of anchored reinforcing bars, ACI Structural Journal, 1997, 94(2), 248-261.

[7] OH B. H. Flexural analysis of reinforced concrete beams containing steel fibers, Journal of Structural Engineering, ASCE, 1992, 118(10), pp.2821-2836.

[8] Park, R., Kent, D. C. and Sampson, R. A. (1972) "Reinforced concrete members with cyclic loading", *Journal of the Structural Division, ASCE*, Vol. 98 ST7, pp. 1341-1360

[9] SAATCIOGLU M., ALSIWAT J. M. and OZCEBE G. Hysteretic behavior of anchorage slip in RC members, Journal of Structural Engineering, ASCE, 1992, 118(9), 2439-2458.

[10] Takeda, T., Sozen, M. A., and Nielsen, N. N. (1970) "Reinforced Concrete Response to Simulated Earthquake" *Journal of the Structural Division, ASCE*, 96(ST-12), 2557-2573.

[11] Taucer, T., Spacone, E. and Filippoou, F. C. (1991) "A fiber beam-column element for seismic response analysis of reinforced concrete structures", *Earthquake Engrg. Research Center Report No. EERC 91-17,* Univ. of California, Berkeley, Calif.

[12] Wight, J. K. and Sozen, M. A. (1975) "Strength decay of RC columns under shear reversals", *Journal of the Structural Division, ASCE,* Vol. 101, No. ST-5, pp. 1053-1065.